DETERMINATION OF OPTICAL CONSTANTS OF A THIN FILM USING ROTATING ANALYZER ELLIPSOMETRY OF MULTIPLE ANGLE OF INCIDENCE

By

Abraham Aklog

SUBMITTED IN PARTIAL FULFILLMENT OF THE
REQUIREMENTS FOR THE DEGREE OF
MASTER OF SCIENCE
AT
ADDIS ABABA UNIVERSITY
ADDIS ABABA, ETHIOPIA
JUNE 2006

© Copyright by Abraham Aklog, 2006

ADDIS ABABA UNIVERSITY
DEPARTMENT OF
PHYSICS

The undersigned hereby certify that they have read and recommend to the Faculty of Science for acceptance a thesis entitled "**Determination of optical constants of a thin film using rotating analyzer Ellipsometry of multiple angle of incidence**" by **Abraham Aklog** in partial fulfillment of the requirements for the degree of **Master of Science**.

Dated: June 2006

Supervisor: ______________________
Dr. Araya Asfaw

Examiners: ______________________
Dr. Mesfin Redi

____
Prof. A.V.Gholap

ADDIS ABABA UNIVERSITY

Date: **June 2006**

Author: **Abraham Aklog**

Title: **Determination of optical constants of a thin film using rotating analyzer Ellipsometry of multiple angle of incidence**

Department: **Physics**

Degree: **M.Sc.** Convocation: **June** Year: **2006**

Permission is herewith granted to Addis Ababa University to circulate and to have copied for non-commercial purposes, at its discretion, the above title upon the request of individuals or institutions.

Signature of Author

THE AUTHOR RESERVES OTHER PUBLICATION RIGHTS, AND NEITHER THE THESIS NOR EXTENSIVE EXTRACTS FROM IT MAY BE PRINTED OR OTHERWISE REPRODUCED WITHOUT THE AUTHOR'S WRITTEN PERMISSION.

THE AUTHOR ATTESTS THAT PERMISSION HAS BEEN OBTAINED FOR THE USE OF ANY COPYRIGHTED MATERIAL APPEARING IN THIS THESIS (OTHER THAN BRIEF EXCERPTS REQUIRING ONLY PROPER ACKNOWLEDGEMENT IN SCHOLARLY WRITING) AND THAT ALL SUCH USE IS CLEARLY ACKNOWLEDGED.

to Thursday

A day everything seems to flow perfectly

Table of Contents

Table of Contents v

List of Tables vii

List of Figures viii

Abstract x

Acknowledgements xi

Introduction 1

1 Introduction 4

1.1 Historical Development of the Concept of Light 4
1.2 Maxwell Equations and Boundary Conditions 7
1.3 Polarization 10
1.3.1 Formal Description of Polarized Light 10
1.4 Modern Description of Polarized and Unpolarized Light 13
1.4.1 Poincarè Sphere 13
1.5 Stokes Vectors 15
1.6 Jones Vectors and Matrices 16
1.6.1 Mueller Formalism 19

2 Ellipsometry 21

2.1 Overview 21
2.2 Theoretical Background of Ellipsometry 22
2.2.1 Definition of Ellipsometric Quantities 22
2.2.2 Reflection by an Ambient Film Substrate System 24

2.3 Photometric Ellipsometry . . . 27
2.3.1 Ellipsometric Equations for RAE . . . 29
2.4 Multiple Angle of Incidence Ellipsometry . . . 31

3 Experimental Setup and Procedure **33**
3.1 Preparation and Nature of the Sample . . . 33
3.2 Basic Principle of Operation of RAE . . . 34
3.2.1 Instrumentation of Rotating Analyzer Ellipsometry . . . 34
3.2.2 Calibration of Rotating Analyzer Ellipsometry . . . 37
3.3 Measurement and Procedure . . . 38

4 Results, Analysis and Discussion **40**
4.1 Simulation and Numerical Inversion of Ellipsometric Data . . . 40
4.2 Parameters Correlation Test . . . 42
4.3 Data from Brewster Angle Measurement . . . 43
4.4 Results for Optical Parameters of MDMO-PPV/PCBM[1:1] . . . 45
4.5 Data from the Absorption Spectrum . . . 47
4.6 Error Analysis . . . 49

5 Conclusion and Recommendations **53**
5.1 Conclusion . . . 53
5.2 Recommendations . . . 54

Appendix **55**

Bibliography **58**

List of Tables

1.1 *Mueller matrices for several components that are often used in ellipsometry.* 20

2.1 *Advantage and disadvantage in several photometric ellipsometer types.* 28

4.1 *Test for the correlation of the optical parameters for MDMO-PPV/PCBM[1:1] at 532nm.* 42

4.2 *Computed ellipsometric quantities from numerical inversion and measured ellipsometric quantities from the Fourier coefficients.* 46

4.3 *measured optical constants and thickness of MDMO-PPV/PCBM[1:1].* 50

List of Figures

1.1 *reflection and transmission of a plane wave at the planar interfaces between two semi-infinite media 0 and 1* 9

1.2 *Elliptically polarized light for arbitrary phase shift.* 12

1.3 *Poincarè sphere.* 13

1.4 *Schematic diagram for incident and output plane waves of Jones vectors* 18

2.1 *An interpretation of* Δ *and* Ψ *upon reflection of a linearly polarized at an interface A between two media* 23

2.2 *Multiple reflection and transmission of a plane wave by ambient-film-substrate system.* 24

3.1 *standard rotating analyzer ellipsometer (RAE) in which polarizer is maintained at a fixed angle and compensator is absent* 35

3.2 *Automated ellipsometer setup.* 36

3.3 *Reflected intensity for S-polarized incident light versus analyzer angle for glass.* 38

4.1 *Reflected intensity* (R_p) *versus analyzer angle for glass substrate* . . . 43

4.2 *Reflected intensity* (R_p) *versus angle of incidence* (θ) *for ambient-film-substrate* 44

4.3 *Intensity versus analyzer angle for five angles of incidence at wavelength 532nm.* 45

4.4 *Intensity versus analyzer angle for five angles of incidence at wavelength 808nm.* 47
4.5 *Absorbance from UV/Vis spectrometer and Ellipsometry measurement.* 48
4.6 *Intensity versus analyzer angle for five angles of incidence at wavelength 1064nm.* 52
4.7 *Intensity versus analyzer angle for five angles of incidence at wavelength 632.8nm.* 52

Abstract

With multiple angle of incidence rotating analyzer ellipsometry, one can measure complex refractive index and the thickness of a very thin film simultaneously. This method is applied on conducting thin film polymer (MDMO-PPV/PCBM[1:1]) for five angles of incidence. In general, it is not possible to invert the Fresnel equations to obtain the complex index parameters, instead, the optical method has to be developed. In the model, the optical parameters are varied to minimize some chosen error function. And those parameters which give a minimum error function are taken to be the correct optical constants of the sample. Additional data are also gathered from absorption measurement, and the two independent measurements are compared. The complex refractive index and thickness of the sample for wavelengths 532 nm, 632.8 nm, 808 nm and 1064 nm are determined.

Acknowledgements

I am very grateful to Dr. Araya Asfaw, my advisor, who inspires me to develop the habit of team work in a research. As a beginner experimentalist, it helps a lot to develop my confidence to engage myself in a more advanced research. I thank the polymer research group of physics department for supplying the sample for the experiment. Finally, I greatly appreciate the technical assistance Tesfaye Mamo offered me.

Abraham Aklog

June 27, 2006

Introduction

Ellipsometry is a technique that has been studied for several centuries. However, it has recently found much favor in the non-destructive characterization of solids, particularly, semiconductors. Ellipsometry can generally be defined as the process of measurement and analysis of the elliptical polarization of light. Ellipsometry (reflection) measures the change in the state of polarization of light upon reflection from a surface. The fact changes are measured rather than the absolute intensity of the light renders ellipsometry sensitive to sub mono layer surface coverage.
There are two major kinds of ellipsometry widely used nowadays. These are spectroscopic ellipsometry (SE) and multiple angle of incidence (MAI) ellipsometry. In SE, the complex reflection ratio is measured over a range of wavelength at a fixed angle of incidence. In MAI Ellipsometry the angle of incidence is varied over range of angles which are particularly grouped around the principal angle. MAI system, generally, but necessarily, employs lasers as the light source. Lasers are highly monochromatic and have a much higher intensity at specific wavelength than conventional source. Furthermore, the beam divergence is minimum. This reduces systematic errors in MAI systems.
In this project, MAI ellipsometry is used to determine the complex refractive index and thickness of a spin coated MDMO-PPV/PCBM[1:1] polymer. A new setup of

ellipsometer is automated and interfaced with acquisition software. The setup is a rotating analyzer ellipsometry. The reflected intensity is analyzed by rotating the analyzer for four wavelengths (532 nm, 632 nm, 808 nm and 1064 nm).

Fresnel equations are difficult to invert. Therefore, an optical model is required to get the complex index parameters. The model consists of isotropic thin film on a substrate. The complex index of refraction of the film and substrate, and film thickness are varied till a best fit is achieved. The fitting process uses a numerical inversion method (written in FORTRAN) with a suitable guess of the optical constants.

The thesis is structured as follow:

> Chapter one introduces the theoretical basis of light wave. In this chapter, Maxwell equations and boundary conditions are briefly treated. Different approaches for representation of polarization of light wave is thoroughly considered.
>
> Chapter two is the main frame of the project report. The basic theory of ellipsometry is fully developed and different kinds of ellipsometry are presented. Emphasis is made on a rotating analyzer ellipsometry. Mueller formalism is used to calculate the behavior of RAE ellipsometer.
>
> In chapter three, the nature of the sample and instrumentation of ellipsometer are described.
>
> Chapter four is devoted to the simulation of ellipsometric quantities and analysis of optical parameters. The optical parameters of the polymer is determined using the optical model developed. Different errors associated with determined optical parameters are considered. The absorbance

of the sample by UV/Vis spectrometer is compared with the results obtained from the ellipsometric measurement.

Finally, conclusion from the preceding chapters are summarized and recommendations are made for future efforts in further development of ellipsometer in Advanced Optics Lab.

Chapter 1

Introduction

1.1 Historical Development of the Concept of Light

The question 'what is light?' immutably remains while the answer subtly changes through time. The search for the explanation of the property of light dates back to remote antiquity. The rectilinear propagation of light, as well as law of reflection, was explained by Euclid in 300 B.C. [1].

From seventeenth century onward, a number of laws and theories are proposed for light. The discovery of the law of refraction by Willebroad Snell in 1621 was one of the greatest moment in optics.

The actual nature of light, particle or wave comes to the picture of contemporary physicists in the seventeenth century. Sir Isaac Newton, one of the greatest physicists, proposed a corpuscular theory of light. He concluded that white light is composed of a mixture of particles. Contrary to Newton, C. Huygens advocated the wave theory of light. Using wave theory, he was able to derive laws of reflection and refraction. He was also able to discover the phenomenon of polarization. Despite this, the corpuscular theory of light dominated the wave theory during eighteenth century.

The wave theory of light was reborn at hands of Pr.Thomas Young. He was able

to explain colored fringes of thin films and determined wavelength of various colors using Newton's data. This is an interference phenomena. A.J. Fresnel, unaware of the efforts of Young, also independently developed wave theory of light. He was able to calculate the diffraction patterns. Fresnel went on to evolve to calculate a mechanistic description of aether oscillation, which led to his famous formulas for amplitudes of reflected and transmitted light. The polarization phenomenon demands that the light wave phenomenon as described by transverse with this breaking discovery, by 1825 corpuscular theory had only a few tenacious advocates.

One of the fascinating problems of measurement in experiment was determination of the speed of light. The first terrestrial determination of speed of light was performed by A.H.L. Fizeau in 1849. Using rotating mirror arrangement in order to measure the duration of an electric spark, Arago reported to the academy of science that the speed of light in water is less than the speed in air. This surprising result at that time shakes strongly held Newton's formulation of the corpuscular theory. Quite independently, the magnetism and electricity was studied thoroughly by experimentalist Michael Faraday. Faraday established an interrelationship between electromagnetism and light when he found that polarization direction of a beam could be allowed by a strong magnetic field applied to the medium.

One of the greatest breakthrough of Electricity and Magnetism is achieved by James Clerk Maxwell. He elegantly summarized the behavior of electric and magnetic fields in a single set of mathematical equations. From this equation, he successfully solved the speed of light. He predicted that the electromagnetic wave propagates as a transverse wave in the luminiferous aether. This conclusion leads to the fact that light was electromagnetic disturbance in the form of waves propagating through aether.

The acceptance of the wave theory of light seemed to necessitate an equal acceptance of the existence of all pervading substrum, the luminiferous aether. If there were waves, it seemed obvious that there must be a supporting medium. The corpuscular model of light could explain stellar aberration rather handily. Alternatively, the wave theory also offers a satisfactory explanation provided that aether totaly undisturbed as earth plows through it. The Michelson-Morley experiment refuted the concept of aether.

In twentieth century new concepts of explanation of light arises, Quantum mechanics. In 1905, Einstein proposed a new form of corpuscular theory in which he asserted that light consisted of globs or 'particles' of energy. Each such quantum radiant energy is called photon. It gradually, using quantum mechanics, become evident that concept of particle and wave, which in the macroscopic world seem so obviously mutually exclusive must be merged in submicroscopic domain. Experimental result obtained agreed with quantum mechanics prediction.

Many properties of matter are probed by interaction of matter. This branch of physics is spectroscopy. With this tool, many optical properties of a given material are analyzed. The invention of laser greatly enhanced research undergoing on spectroscopy. There are number of techniques used depending on the information required reflectance, RAS, ellipsometry, transmission, Raman scattering and etc.

A far-reaching revolution in the methods of processing and community information is quietly taking, a revolution that will continue to change our lives in the years ahead. On other side theoretical explanation of mysterious light is still keen interest for many scientists.

1.2 Maxwell Equations and Boundary Conditions

Maxwell expressed the results of his theoretical investigation in the form of four fundamental equations which have since become famous as Maxwell's Equations. They were based on the earlier experimental researches of Oersted, Faraday and Joseph Henry concerning the the relations between electricity and magnetism. They summarize these relations in concise mathematical form and constitute a starting point for the investigation of all electromagnetic phenomena. The four Maxwell equations can be expressed in the following way for the case of free space:

$$\nabla.\overrightarrow{D} = \rho_f \tag{1.2.1}$$

$$\nabla.\overrightarrow{B} = 0 \tag{1.2.2}$$

$$\nabla \times \overrightarrow{E} = -\frac{\partial \overrightarrow{B}}{\partial t} \tag{1.2.3}$$

$$\nabla \times \overrightarrow{H} = \overrightarrow{J}_f \tag{1.2.4}$$

The above four equations are sufficient to determine the electromagnetic field completely if ρ_f and $\overrightarrow{J}_f$ are given and the electric properties of the medium are known. For isotropic linear medium, $\overrightarrow{B} = \mu \overrightarrow{H}$ and $\overrightarrow{D} = \varepsilon \overrightarrow{E}$.
Maxwell equations become

$$\nabla.\overrightarrow{E} = \frac{\rho_f}{\varepsilon} \tag{1.2.5}$$

$$\nabla.\overrightarrow{B} = 0 \tag{1.2.6}$$

$$\nabla \times \overrightarrow{E} = -\frac{\partial \overrightarrow{B}}{\partial t} \tag{1.2.7}$$

$$\nabla \times \overrightarrow{B} = \mu \overrightarrow{J}_f + \mu\varepsilon \frac{\partial \overrightarrow{E}}{\partial t} \tag{1.2.8}$$

For no external charge densities and currents

$$\overrightarrow{J}_f = \sigma_c \overrightarrow{E}$$

$$\nabla \times \overrightarrow{B} = \mu\sigma_c \overrightarrow{E} + \mu\varepsilon \frac{\partial \overrightarrow{E}}{\partial t} \quad (1.2.9)$$

where σ_c is conductivity of the material

μ is permeability of the material

ϵ is the permittivity of the material

This relations yield to a three-dimensional wave equations which are expressed by

$$\nabla^2 \overrightarrow{E} = \mu\sigma_c \frac{\partial \overrightarrow{E}}{\partial t} + \mu\varepsilon \frac{\partial^2 \overrightarrow{E}}{\partial t^2} \quad (1.2.10)$$

$$\nabla^2 \overrightarrow{B} = \mu\sigma_c \frac{\partial \overrightarrow{B}}{\partial t} + \mu\varepsilon \frac{\partial^2 \overrightarrow{B}}{\partial t^2} \quad (1.2.11)$$

The solution of the above equations have septile complex form

$$\overrightarrow{E} = \hat{E} e^{-i(\omega t - \overrightarrow{k}.\overrightarrow{r})}, \qquad \overrightarrow{B} = \hat{B} e^{-i(\omega t - \overrightarrow{k}.\overrightarrow{r})}, \quad (1.2.12)$$

where $\hat{E}$ and $\hat{B}$ are complex vector amplitudes independent of $\overrightarrow{r}$ and t. When light passes from one medium in to another EMF vectors must satisfy boundary condition. The boundary condition is the continuity of the tangential components of $\overrightarrow{E}$ and $\overrightarrow{H}$ vectors on the interface between the two isotropic media. The incident electric field $\overrightarrow{E}$ can be decomposed into two orthogonal components. The component perpendicular to the plane of incidence is S-component, and the component parallel to the plane of incidence is P-component. From boundary condition, the Fresnel reflection and transmission coefficients for S- and P-polarization can be derived.

$$r_p = \frac{E'_{0p}}{E_{0p}} = \frac{n_1 \cos\theta_0 - n_0 \cos\theta_1}{n_1 \cos\theta_0 + n_0 \cos\theta_1}. \quad (1.2.13)$$

$$t_p = \frac{E_{1p}}{E_{0p}} = \frac{2n_0 \cos\theta_0}{n_1 \cos\theta_0 + n_0 \cos\theta_1} \quad (1.2.14)$$

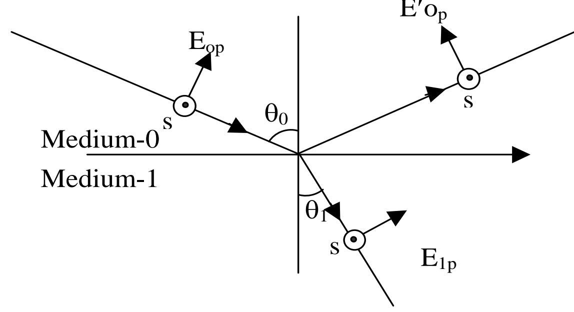

Figure 1.1: *reflection and transmission of a plane wave at the planar interfaces between two semi-infinite media 0 and 1 .*

$$r_s = \frac{E'_{0s}}{E_{0s}} = \frac{n_0 \cos\theta_0 - n_1 \cos\theta_1}{n_0 \cos\theta_0 + n_1 \cos\theta_1} \tag{1.2.15}$$

$$t_s = \frac{E_{1s}}{E_{0s}} = \frac{2n_0 \cos\theta_0}{n_0 \cos\theta_0 + n_1 \cos\theta_1} \tag{1.2.16}$$

and Snell's law for the two systems,

$$n_0 \sin\theta_0 = n_1 sin\theta_1, \tag{1.2.17}$$

where n_0 and n_1 are indices of refraction of the two media.

When a P-polarized light wave is incident on the interface between two transparent media, the reflected wave entirely disappears at a particular angle of incidence called the Brewster angle ϕ_B, and the incident is totally refracted into the second medium. Setting $r_p = 0$ and using equation (1.2.17),

$$\tan\phi_B = (n_1/n_0). \tag{1.2.18}$$

1.3 Polarization

An oscillating vector field must instantaneously have a unique direction. For the plane electromagnetic wave in an isotropic medium this direction must be perpendicular to the wave normal; if it remains constantly in the same direction, the wave is said to be Plane polarized. On the other hand, if the direction changes randomly, the wave is said to be unpolarized or randomly polarized.

Depending on the phase difference between two oscillating electric field vectors, we can have a linear, circular or elliptical polarization. Two plane polarized waves can combine to produce another wave which is also plane polarized.

If the phase difference is a multiple of $\pi/2$, the resultant oscillating vector now rotates following a circle or ellipse depending on the amplitudes of the two vectors. Linearly polarized light is a surprisingly common phenomenon in everyday circumstances. Light reflected from any smooth surfaces such as a wet road or a polished table top, partially linearly polarized; this is easily demonstrated by turning the polaroid glass which gives a change in brightness according to the change in angle between the plane of polarization and the transmission axis of the polaroid. The maximum effect is found for reflection at a particular angle of incidence, the Brewster angle.

1.3.1 Formal Description of Polarized Light

When light interacts with matter, the force exerted on the electron by the electric field of the light wave is much greater than the magnetic field. That is why the polarization is determined by the direction of electric field.

Let us consider an electromagnetic wave propagating along $\hat{x}$ direction. The orthogonal electric fields are along $\hat{y}$ and $\hat{z}$ axes. These components are the two plane

polarized waves. There is a phase difference ϕ between the two components.

$$\overrightarrow{E_y} = E_{0y} \exp i(\omega t - kx)\hat{y} \tag{1.3.1}$$

$$\overrightarrow{E_z} = E_{0z} \exp i(\omega t - kx + \phi)\hat{z} \tag{1.3.2}$$

If we take the real component of the above equations, and taking the electric field at a fixed space $x = 0$

$$\overrightarrow{E_y} = E_{0y} \cos(\omega t)\hat{y}$$
$$\overrightarrow{E_z} = E_{0z} \cos(\omega t + \phi)\hat{z}$$

Taking the magnitude of $\overrightarrow{E_y}$ and $\overrightarrow{E_z}$

$$\frac{|\overrightarrow{E_y}|}{E_{oy}} = \cos(\omega t)$$
$$\frac{|\overrightarrow{E_z}|}{E_{oz}} = \frac{|\overrightarrow{E_y}|}{E_{oy}} \cos(\phi) - \sin(\omega t)\sin(\phi)$$

Squaring both side and simplifying,

$$\frac{|\overrightarrow{E_z}|^2}{E_{oz}^2} + \frac{|\overrightarrow{E_y}|^2}{E_{oy}^2} - 2\frac{|\overrightarrow{E_y}||\overrightarrow{E_z}|}{E_{oy}E_{oz}} cos(\phi) = \sin^2(\phi). \tag{1.3.3}$$

This is the general equation of ellipse. Depending on the values of ϕ, the equation can represent line, circle or ellipse. The sign of ϕ determines the sense of rotation.

Case I. When the phase difference is an integral multiple of π, equation(1.3.3) becomes

$$E_y = \pm \frac{A_y}{A_z} E_z$$

The wave is linearly polarized. The negative sign is when it is an odd multiple of π and the positive sign is when it is an even multiple of π.

Case II. When phase difference is an odd multiple of $\pi/2$ and $E_{oy} = E_{oz}$, equation(1.3.3) represents an equation of a circle.

$$E_y^2 + E_z^2 = A^2$$

This is a circularly polarized light, a given vector precess with a constant angular speed with constant magnitude. When z-component electric field leads y-component, we have clockwise rotation which is called right handed polarization.

Case III. When the phase difference is an odd multiple of $\pi/2$ and $E_{oz} \neq E_{oy}$, the polarization becomes elliptic whose major axis lies either on y or x axis.

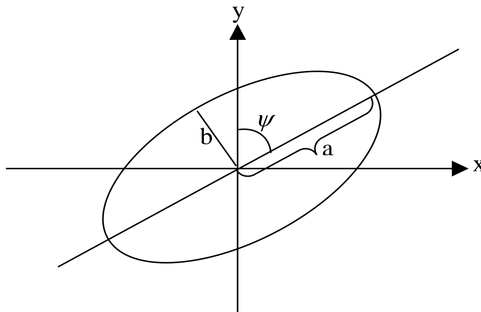

Figure 1.2: *Elliptically polarized light for arbitrary phase shift.*

Case IV. For a general case, when ϕ is not an integral multiple of$\pi/2$, elliptical polarization whose major axis does not lie along z or y will result. The tilting angle ψ is defined as

$$\tan(2\psi) = \frac{2ab\cos(\phi)}{a^2 - b^2}$$

Ellipticity e is the ratio of the length of the semi-minor axis of the ellipse b to the length of semi- major axis a. The right-handed and left-handed circularly polarized states correspond to $e = 1$ and $e = -1$ respectively. Linearly polarized light has

ellipticity of zero magnitude.

1.4 Modern Description of Polarized and Unpolarized Light

1.4.1 Poincarè Sphere

The Poincarè sphere is a unit radius spherical surface each point of which signifies a different polarization form [2]. It is a polarization space in the form of a spherical surface whose points are a one to one correspondence with different states of polarizations of light. The state of polarization of light can be described by using different kinds of polarization space. The complex plane representation of polarized light gives another space whose points are in one to one correspondence with different possibilities of polarization.

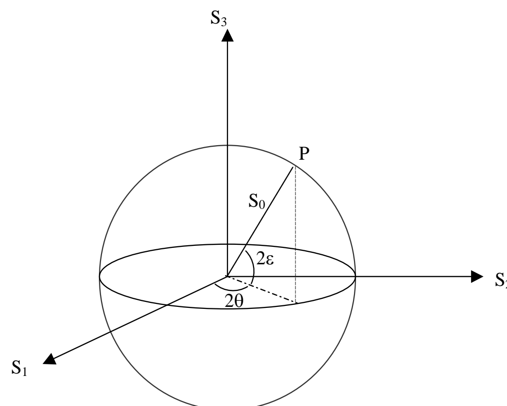

Figure 1.3: *Poincarè sphere.*

Consider a sphere of radius S_0. Any point on the sphere is represented by longitude 2θ and latitude 2ϵ. The following properties of polarized light can be associated with a point P on a sphere.

1. The north and the south pole stands for the left and right circular polarization respectively.
2. Every point on the equator represents a linear polarization form; each point implies different oscillation direction.
3. The northern hemisphere excluding the north pole represents right handed elliptical polarization and the southern hemisphere excluding the south pole represents left handed elliptical polarization.
4. The latitude whose common axis is polar axis from south to north pole represents an equiellipticity contour.

In general, the state of polarization is described by azimuthal ψ and ellipticity angle as described in the previous section. These two quantities represent a point on the Poincarè sphere with a coordinate of latitude 2ϵ and the longitude 2θ. A bilinear transformation can be produced from the Poincarè sphere representation to a cartesian coordinate system. A given point P is represented with a spherical coordinate $(S_0, \pi/2 - 2\epsilon, 2\theta)$. This can be expressed in a new cartesian coordinate system (see figure 1.3).

$$S_0^2 = S_1^2 + S_2^2 + S_3^2 = E_x^2 + E_y^2, \tag{1.4.1}$$

$$S_1 = S_0 \cos(2\epsilon)\cos(2\theta) = {E_x}^2 - {E_y}^2, \tag{1.4.2}$$

$$S_2 = S_0 \cos(2\epsilon)\sin(2\theta) = 2E_x E_y \cos\phi, \tag{1.4.3}$$

$$S_3 = S_0 \sin(2\epsilon) = 2E_x E_y \sin\phi, \tag{1.4.4}$$

where ϕ is the phase shift between the horizontal and the vertical components of the electric field $\overrightarrow{E}$ propagating in z direction .

If the radius of the Poincarè sphere is unity, the above equations represent Stokes parameters.

1.5 Stokes Vectors

[3] In 1852 G.G. Stokes introduced four quantities, Stokes parameters, which are functions of the observable electromagnetic waves. It equally applies well to polarized light, partially polarized light and unpolarized light. Stokes vector is a 4×1 column of vector consisting of Stokes parameters. In order to exploit the use of compact matrix formalism to investigate the interaction between the the light wave and the optical components, Stokes vectors is preferred to Poincarè sphere representation. It is often written horizontally to save space. Stokes parameters are a set of four real quantities with dimension of intensity given by equations(1.4.1-1.4.4)

The first parameter S_0 is the total intensity of the light waves. S_1 gives the difference between x and y components and can be either positive, negative or zero. It reduces to positive when the vibration is horizontal and reduces to negative when the vibration is vertical. It becomes zero when the beam is circularly polarized, elliptically polarized with major axis is at $\pm\pi/4$ or unpolarized. Thus it does indicate preference of x polarization to y polarizations. Stokes parameter S_3 represents the preference of the wave to either right or left handed circularly polarized component. The third component S_2 represents a preference for $\pm\pi/4$ linear polarization.

When a given light is completely polarized, the following relation holds.

$$S_0^2 = S_1^2 + S_2^2 + S_3^2.$$

For partially polarized light, the relation becomes,

$$S_0^2 > S_1^2 + S_2^2 + S_3^2.$$

The degree of polarization is the ratio of the intensity of totally polarized light to the total intensity of the light. Mathematically, it is given as,

$$P = \frac{S_1^2+S_2^2+S_3^2}{S_0^2}.$$

It is important to remember that Stokes vectors may be added only when the beams concerned are incoherent [4].

1.6 Jones Vectors and Matrices

Jones vector is an abstract mathematical space formed by all vectors that are obtained by considering all possible pairs of complex numbers for $\overrightarrow{E_x}$ and $\overrightarrow{E_y}$. It is a two elements column vector. Each element describes one component of electric field $\overrightarrow{E}$. It is superior to the Stokes vector in some ways and inferior in others. It is superior in that, it is applicable to the addition of coherent beams; also it is more compact. But it can not handle unpolarized or partially polarized light.

Consider a uniform transverse electric elliptically polarized plane wave. If such a wave is assumed to propagate in z-direction, $\overrightarrow{E}$ is given by

$$\overrightarrow{E}(z,t) = \tilde{E}_x cos(wt - 2\pi z/\lambda + \delta_x)\hat{x} + \tilde{E}_y cos(wt - 2\pi z/\lambda + \delta_y)\hat{y}, \qquad (1.6.1)$$

where $\tilde{E}_x$ and $\tilde{E}_y$ represent amplitudes of the linear, simple harmonic oscillation of the electric field components along the x and y axes, and σ_x and σ_y represent the respective phases of the oscillation.

A more compact mathematical description of the wave can be obtained from equation(1.6.1). This compact description is sufficient enough to fully explain the wave polarization and its modification after interacting with optical optical devices. The concise description is the Jones vector of a wave represented by the following matrix.

$$\overrightarrow{E} = \begin{pmatrix} \tilde{E}_x e^{(i\sigma_x)} \\ \tilde{E}_y e^{(i\sigma_y)} \end{pmatrix} \tag{1.6.2}$$

From the above equation, the Jones vectors for different polarization can be obtained.

1. For linearly polarized light wave, the normalized Jones vector is

$$\overrightarrow{E} = \begin{pmatrix} \cos\theta \\ \sin\theta \end{pmatrix}$$

   where θ is the angle the vector makes with the x-axis.

   Particularly for x-polarization and y-polarization, the Jones vectors become $\begin{pmatrix} 1 \\ 0 \end{pmatrix}$, and $\begin{pmatrix} 0 \\ 1 \end{pmatrix}$

2. For left and right circularly polarized light, the normalized Jones vectors are respectively

$$\overrightarrow{E}_l = \tfrac{1}{\sqrt{2}} \begin{pmatrix} 1 \\ -i \end{pmatrix}$$

$$\overrightarrow{E}_r = \tfrac{1}{\sqrt{2}} \begin{pmatrix} 1 \\ i \end{pmatrix}$$

The main use of Jones vector is in computing the effect of inserting optical devices like polarizer, analyzer and retarder in a given system. This effect easily computed by multiplying Jones vectors of incident beam by respective Jones matrices of the optical devices. The optical elements are represented by 2×2 Jones matrix.
Consider an incident wave on a non depolarizing optical system that consists of a single optical device. Due to the interaction, a modified wave will emerge from the system. This is shown in following schematic diagram. The incident and the out

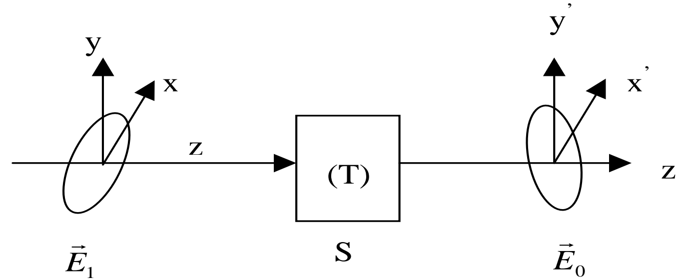

Figure 1.4: *Schematic diagram for incident and output plane waves of Jones vectors*

going plane waves can be described by their appropriate Jones vectors $\overrightarrow{E_1}$ and $\overrightarrow{E_0}$. These two plane waves are related by a linear relation,

$$E_{0x} = T_{11}E_{1x} + T_{12}E_{1y}. \tag{1.6.3}$$

$$E_{0y} = T_{21}E_{1x} + T_{22}E_{1y}. \tag{1.6.4}$$

This can be written in a more compact form by matrix,

$$E_0 = TE_1, \text{ where } T = \begin{pmatrix} T_{11} & T12 \\ T_{21} & T_{22} \end{pmatrix}$$

The 2×2 transformation matrix T is called Jones matrix of the optical device. [12] It includes the overall effect of optical devices on the incident wave.

This result can be generalized for a series of successive optical devices.The out going light is given for such system simply as,

$$E_0 = T_n T_{n-1} ... T_1 T_0 E_1,$$

where T_n represents Jones matrix of the nth optical device.

1.6.1 Mueller Formalism

[5] For partially polarized quasi-monochromatic light, Jones formalism fails. The reason is that a deterministic 2×2 complex Jones matrix can no longer be used to express the depolarizing incoherent interaction between incident wave and the optical system. A more general formalism is required to handle such a general case. This more powerful tool is Mueller calculus. The outgoing Stokes vector S_i and the incident Stokes vector S_0 are related,

$$S_0 = M S_i, \tag{1.6.5}$$

where M is 4×4 Mueller matrix. Equation (1.6.5) gives the basic law of transformation of Stokes vector of a partially polarized light wave as it propagates though optical system. This procedure can be repeated, and a complete train of optical components may be described by one Mueller matrix, which is a product of the separate components of Mueller matrices.

If the incident light is totally polarized and the optical system is non-depolarizing, the Mueller matrix formalism can not be used to investigate information on the absolute phase of the wave. This is easily explained as Stokes vector does not include

Optical component	Mueller matrix
1. A perfect linear polarizer with horizontal transmission axis	$\frac{1}{2}\begin{bmatrix} 1 & 1 & 0 & 0 \\ 1 & 1 & 0 & 0 \\ 0 & 0 & 0 & 0 \\ 0 & 0 & 0 & 0 \end{bmatrix}$
2. A partial linear polarizer with horizontal transmission axis and attenuation coefficient α	$\frac{1}{2}\begin{bmatrix} 1+\alpha & 1-\alpha & 0 & 0 \\ 1-\alpha & 1+\alpha & 0 & 0 \\ 0 & 0 & 2\sqrt{\alpha} & 0 \\ 0 & 0 & 0 & 2\sqrt{\alpha} \end{bmatrix}$
3. Ellipsomertic reflection sample where the major axis is determined by the plane of incidence	$\begin{bmatrix} 1 & -\cos 2\Psi & 0 & 0 \\ -\cos 2\Psi & 1 & 0 & 0 \\ 0 & 0 & \sin 2\Psi \cos\Delta & \sin 2\Psi \sin\Delta \\ 0 & 0 & -\sin 2\Psi \sin\Delta & \sin 2\Psi \cos\Delta \end{bmatrix}$
4. A matrix to represent a component in another fame of reference rotated over angle θ relative to the old frame of reference.	$\frac{1}{2}\begin{bmatrix} 1 & 0 & 0 & 0 \\ 0 & \cos 2\theta & \sin 2\theta & 0 \\ 0 & -\sin 2\theta & \cos 2\theta & 0 \\ 0 & 0 & 0 & 1 \end{bmatrix}$

Table 1.1: *Mueller matrices for several components that are often used in ellipsometry.*

the absolute phase information of the wave. Therefore, the Jones matrix formalism has to be used in this case.

Although the Jones formalism is applicable to coherent light, the Mueller formalism has gradually gained more and more attention. There are several reasons for this. Unlike Jones matrix, Mueller matrix deals directly with observable quantities. So, there are no complex number involved in Mueller formalism. Mueller formalism can handle a partially polarized light. Because of the use of computer in algebra a 4×4 Mueller matrix are as easy to handle as a 2×2 Jones matrix [6].

Chapter 2

Ellipsometry

2.1 Overview

According to Azzam and Bashara, [7] ellipsometry can generally be defined as the measurement of the state of polarization of a polarized wave, and it is solely conducted to obtain characteristic information about the optical system under investigation. The interaction of polarized light with the optical system results in a change of polarization of the light wave. This change of state of polarization can be related to the initial state of polarization and optical properties of the optical system under study. The optical system acts as the transformation matrix that changes the initial states of the polarization to a final one. This transformation can elegantly be handled by Jones or Mueller matrix under different circumstances. The major branch in ellipsometry deals with reflection experiment [8], this paper is solely devoted to this method. But there are many applications of ellipsometry in transmission experiments (polarimetry [9]) and scattering experiments(scattering ellipsometry [10]). Compared to other methods, ellipsometry is preferred because it can be used in real time and in situ

measurement. Ellipsometry is non perturbing, very sensitive, inexpensive, doesn't require ultrahigh vacuum conditions, and with the advance of powerful computer it has become much easier to handle.

Ellipsometry can be applied to a vast area of interest. Its applications ranges from optics to medicine. The optical parameters of a thin films like polymer, silicon, gold etc. can be precisely measured. Using this method, the properties of semiconductors can be studied. It has been a vital probe of electrochemical electrode. Recently, there has been an application of ellipsometry to biology and medicine which gives promising results. In this chapter, the basic ellipsometry quantities will be defined. This is followed by more general consideration of reflection and transmission from stacked two layer system. Furthermore, the photometric ellipsometry will be introduced under this section. Different photometric ellipsometry is discussed and more emphasis is given to a rotating analyzer ellipsometry. At the end of the chapter, the multiple angle of incidence ellipsometry is presented.

2.2 Theoretical Background of Ellipsometry

2.2.1 Definition of Ellipsometric Quantities

The two ellipsometric quantities are ellipsometric angles Ψ and Δ. Although from the point of view of modeling ellipsometric measurement data other quantities, like Fourier coefficients, are to be preferred over the traditional Ψ and Δ, they are still in use. The main reason for this is that these quantities are directly related to the optical parameters of sample under study. To fully grasp this, consider the Fresnel reflection

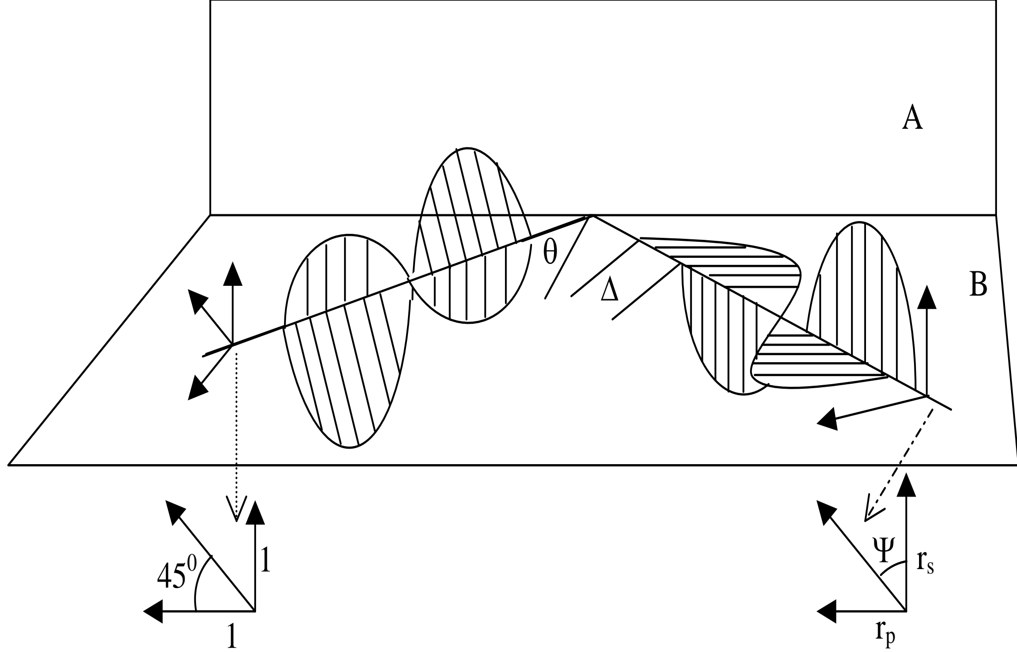

Figure 2.1: *An interpretation of Δ and Ψ upon reflection of a linearly polarized at an interface A between two media*

coefficients [11] for ambient substrate system and observe figure(2.2.1). The plane of incidence B is determined by the incident and reflected light beams.The P-direction is defined parallel to the plane of incidence. The S- component is perpendicular to the plane of incidence.

$$r_p = \frac{n_1 cos(\theta_0) - n_0 cos(\theta_1)}{n1 cos(\theta_0) + n_0 cos(\theta_1)} \tag{2.2.1}$$

$$r_s = \frac{n_0 cos(\theta_0) - n_1 cos(\theta_1)}{n_0 cos(\theta_0) + n_1 cos(\theta_1)} \tag{2.2.2}$$

where θ_0, θ_1, n_0 and n_1 are angle of incidence, angle of refraction, refractive index of ambient and substrate respectively. The reflection coefficients may be interpreted as the eigenvalues of two eigen polarization of reflection. The new complex quantity ρ is

defined as the ratio of the two complex Fresnel reflection coefficients. This quantity measures the change of polarization after interaction with the optical system. It is usually written in polar form as a function of the two ellipsometric angles Ψ and Δ as follows

$$\rho = tan(\Psi)\exp(i\Delta). \tag{2.2.3}$$

From this equation, it is easily seen that tangent of Ψ and the angle $\Delta(0 \leq \Psi \leq 90^0, 0 \leq \Delta \leq 360^0)$ are the relative amplitude change and phase shift between two orthogonal polarization directions, respectively

2.2.2 Reflection by an Ambient Film Substrate System

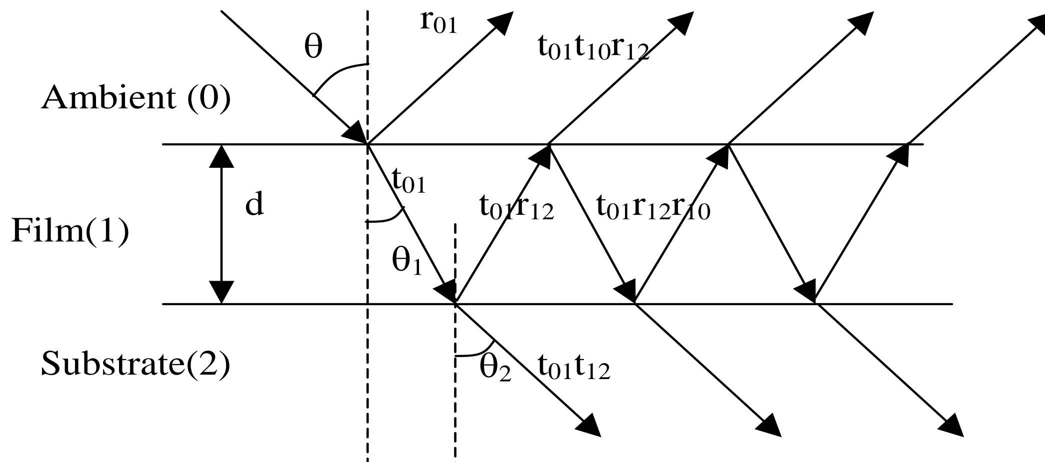

Figure 2.2: *Multiple reflection and transmission of a plane wave by ambient-film-substrate system.*

Now consider a plane electromagnetic waves propagating in ambient(0) and reflecting at angle θ_0 at a system consisting of substrate(2) and layer(1) shown in figure2.2.

The ambient, layer and substrate are all homogeneous and optically isotropic, with complex indices of refraction n_0, n_1 and n_2 respectively. If the substrate is transparent, the n_0 is real. Considering only the S-component of incident light, the reflected wave will only have S-component. The reflected wave inside the layer suffers multiple internal reflections at 1-2 and 1-0 film bounding interfaces. The multiple reflections lead to an infinite geometric series for the total reflected amplitude R_s which is given by

$$R_s = r_{01s} + t_{01s}t_{10s}r_{12s}\exp(-i2\beta) + t_{01s}t_{10s}r_{10s}r_{12s}^2\exp(-i4\beta) + ..., \tag{2.2.4}$$

where

r_{01s} - Fresnel reflection coefficient for interface 0-1

r_{12s}- Fresnel reflection coefficient for interface 1-2

t_{01s}-Fresnel transmission coefficient for interface 0-1

t_{12s}-Fresnel transmission coefficient for interface 1-2

β - phase thickness defined as

$$\beta = \frac{2\pi d n_1 \cos(\theta_1)}{\lambda}. \tag{2.2.5}$$

After summing infinite geometric series and using the relation $r_{10} = -r_{01}$ and $t_{01}t_{10} = 1 - r_{10}^2$. The result becomes

$$R_s = \frac{r_{01s} + r_{12s}\exp(-2i\beta)}{1 + r_{01s}r_{12s}\exp(-i2\beta)}. \tag{2.2.6}$$

Similarly for P-component

$$R_p = \frac{r_{01p} + r_{12p}\exp(-i2\beta)}{1 + r_{01p}r_{12p}\exp(-i2\beta)}. \tag{2.2.7}$$

The Fresnel reflection and transmission coefficients at 0-1 and 1-2 interfaces are given by

$$r_{01p} = \frac{n_1\cos(\theta_0) - n_0\cos(\theta_1)}{n_1\cos(\theta_0) + n_0\cos(\theta_1)}, \tag{2.2.8}$$

$$r_{12p} = \frac{n_2\cos(\theta_1) - n_0\cos(\theta_2)}{n_2\cos(\theta_1) + n_0\cos(\theta_2)}, \tag{2.2.9}$$

$$r_{01s} = \frac{n_0\cos(\theta_0) - n_1\cos(\theta_1)}{n_0\cos(\theta_0) + n_1\cos(\theta_1)}, \tag{2.2.10}$$

$$r_{12s} = \frac{n_1\cos(\theta_1) - n_2\cos(\theta_2)}{n_1\cos(\theta_1) + n_2\cos(\theta_2)}, \tag{2.2.11}$$

$$t_{01p} = \frac{2n_0\cos(\theta_0)}{n_1\cos(\theta_0) + n_0\cos(\theta_1)}, \tag{2.2.12}$$

$$t_{12p} = \frac{2n_0\cos(\theta_0)}{n_1\cos(\theta_0) + n_0\cos(\theta_1)}, \tag{2.2.13}$$

$$t_{01s} = \frac{2n_0\cos(\theta_0)}{n_0\cos(\theta_0) + n_1\cos(\theta_1)}, \tag{2.2.14}$$

$$t_{12s} = \frac{2n_1\cos(\theta_1)}{n_1\cos(\theta_1) + n_2\cos(\theta_2)}, \tag{2.2.15}$$

The three angles θ_0, θ_1 and θ_3 are related by Snell's law

$$n_0\sin(\theta_0) = n_1\sin(\theta_1) = n_2\sin(\theta_2), \tag{2.2.16}$$

The following pre-conditions must be fulfilled to apply the above formulae to a practical film substrate [12].

1. Lateral dimension of the film must be many times its thickness.

2. The source's band width, beam diameter and degree of collimation, as well as film thickness must be in such away that multiple reflected waves combine coherently.

3. The film material must not be amplifying.

These conditions are met for most practical applications of ellipsometry.

For this system a complex reflection ratio, ρ, is defined as,

$$\rho = \frac{R_p}{R_s} = \tan(\Psi)\exp(i\Delta). \tag{2.2.17}$$

From the above function, it can be seen ρ depends on different parameters $n_0, n_1, n_2, d, \theta_0$ and λ. The ellipsometric quantities Δ and Ψ can be expressed as a function of ρ as follows

$$\psi = \arctan(|\rho(n_0, n_1, n_2, d, \theta_0, \lambda)|). \tag{2.2.18}$$

$$\Delta = arg[\rho(n_0, n_1, n_2, d, \theta_0, \lambda)]. \tag{2.2.19}$$

These functions are quite complicated. Hence, there is a need of iteration using a computer to produce the ellipsometric quantities and compare them to the measured Δ and Ψ. This will be discussed in detail in chapter four.

2.3 Photometric Ellipsometry

There are different kinds of ellipsometry depending how the ellipsometry is arranged and optical components used. The two broad major divisions are null and photometric ellipsometry. Photometric ellipsometry is usually performed by modulating the polarization state of a light beam. Depending on the type of optical components

used for the modulation, there are different kinds of photometric ellipsometry. If a linear polarizer is used, rotating analyzer (RAE [13]) and rotating polarizer (RPE). If a retarder is used, rotating compensator (RCE [14]) and the phase modulation ellipsometry(PME [15]) can be achieved using PME. All these different approaches have their own advantages and disadvantages. This is briefly summarized in table (2.1). In this experiment RAE method is employed.

Type	Advantages	Disadvantage
RAE/RPE	• medium-fast • easy calibration • inexpensive	• inaccurate regions in Δ-range • sensitive to detector polarization (RAE) or source polarization (RPE) • need for DC level
RCE	• medium-fast • self-calibrating • non ambiguous Δ • same accuracy everywhere in ψ-Δ plane • no need for DC level determination of complete Stokes vector possible • insensitive to source and detector polarization	• extra retarder
PME	• Very fast • Insensitive to source and detector polarization	• expensive • ambigious in Δ • extra phase modulator

Table 2.1: *Advantage and disadvantage in several photometric ellipsometer types.*

2.3.1 Ellipsometric Equations for RAE

The arrangement of the optical components of RAE is PSA (polarizer sample analyzer) [16]. The analyzer is continuously rotated around the beam axis and the detected signal I_D is Fourier analyzed. A perfect RAE setup is assumed in the calculation of the detected intensity I_D as function of rotating analyzer angle A. In a perfect RAE set up both the analyzer and polarizer are perfect i.e both optical components totally polarize the light source. Also the detector does not depend on the polarization state of the light source. It measures the intensity present in a polarization state indifferent to the polarization state. The detected intensity is obtained by multiplying the Mueller matrices of the optical components and sample in the setup to a Stokes vector which describes the light source. The unpolarized light, represented by Stokes vector $S_0 = (1, 0, 0, 0)$, passes the optical components in RAE setup. And the final emergent light Stokes vector S_f is sought by multiplying the initial Stokes vector with a series of Mueller matrices of the optical components. First consider the Mueller matrix of each component at a definite azimuthal angle relative to the plane incidence. The light passing through a perfect polarizer at azimuth P must be multiplied by the following matrix

$$R(-P) \cdot M_p \cdot R(P), \tag{2.3.1}$$

Where M_p is a Mueller matrix of a perfect polarizer R(P) and R(-P) are rotation matrices. The rotation matrix brings the component into a reference frame rotated over angle P relative to the plane of incidence.

After interaction with the sample, the light source must be multiplied by Mueller

matrix of the sample under investigation. Here the sample defines the plane of incidence. Therefore, it is not multiplied by any rotation matrices.

Similar to the perfect polarizer, the corresponding transformation matrix for the incident light wave for perfect analyzer is given by

$$R(-A) \cdot M_A \cdot R(A) \tag{2.3.2}$$

where M_A is Mueller matrix of a perfect analyzer.

The final Stokes vector is given by

$$R(-A) \cdot M_A \cdot R(A) \cdot M_{\Psi\Delta} \cdot R(-P) \cdot M_P \cdot R(P) \tag{2.3.3}$$

This equation can further be simplified since the light incident is unpolarized. Unpolarized light is invariant under rotation of the frame of reference. Hence, the first rotation matrix may be dropped out. Since a perfect detector is assumed, the last rotation matrix can also be left out. Therefore, the expression becomes,

$$S_f = M_A \cdot R(A) \cdot M_{\Psi\Delta} \cdot R(-P) \cdot M_P \tag{2.3.4}$$

The intensity, I, is represented by the first component of the Stokes vector S_f.

$$I = (1 - \cos 2\Psi \cos 2P)\left(1 + \cos 2A \frac{\cos 2P - \cos 2\Psi}{1 - \cos 2\Psi \cos 2P} + \sin 2A \frac{\cos\Delta \sin 2\Psi \sin 2P}{1 - \cos 2\Psi \cos 2P}\right) \tag{2.3.5}$$

This is a sinusoidal function. It can simply be written in the following form.

$$I = g(1 + a\cos 2A + b\sin 2A) \tag{2.3.6}$$

If the transmission axis of the polarizer and analyzer lie on y-axis i.e the set up is rotated by 90^0, equation(2.3.6) can be written in the following form.

$$I = g(1 - a\cos 2A - b\sin 2A) \tag{2.3.7}$$

where

$$g = 1 - \cos 2\Psi \cos 2P$$

$$a = -\frac{\cos 2P - \cos 2\Psi}{1 - \cos 2\Psi \cos 2P}, \text{ and}$$

$$b = -\frac{\cos\Delta \sin 2\Psi \sin 2P}{1 - \cos 2\Psi \cos 2P},$$

Using the above equations, the ellipsometric quantities Δ and Ψ can be expressed explicitly in these Fourier coefficients.

$$\cos 2\Psi = \frac{\cos 2P + a}{1 + a\cos 2P} \quad \text{and} \quad \cos\Delta = \frac{-b}{\sqrt{1 + a\cos 2P}} \frac{\sin 2P}{|\sin 2P|}. \tag{2.3.8}$$

If the polarizer is set at an angle of 45^0 relative to the plane of incidence, equation (2.3.8) becomes

$$\cos 2\Psi = a \quad \text{and} \quad \cos\Delta = \frac{-b}{\sqrt{1 - a^2}}. \tag{2.3.9}$$

Therefore, once the Fourier coefficient are obtained from the fitting of experimental data, the ellipsometric angles Δ and Ψ are easily computed using the equation(2.3.9). These ellipsometric quantities characterize the sample under investigation.

2.4 Multiple Angle of Incidence Ellipsometry

Using a fixed angle of incidence, the complex reflection ratio (ρ) is measured over a range of wavelengths. This is generally known as spectroscopic ellipsometry (SE) and is the most widely employed form of ellipsometry. The complex reflectance can be measured for a fixed wavelength over a range of angles of incidence. This method is called multiple angle of incidence (MAI) ellipsometry [17]. The range of angle employed is generally large , but they are particularly grouped around the principal

angle. MAI system generally, but not necessarily, employs laser as the light source. This brings several advantages over conventional light sources. Lasers are highly monochromatic and have a much higher intensity at specific wavelength than the conventional source. Furthermore, they produce highly collimated light; beam divergence is a major systematic error in MAI systems.

When ellipsometric measurement is done on three phase system at one wavelength λ and one angle of incidence, it is only possible to determine two of the optical parameters of the system if all the remaining parameters are known. [18] The ellipsometric measurement at one wavelength λ and one angle of incidence fails to get all information about the optical parameters when the number of unknown optical parameters exceeds two. When such case arises, it is necessary to obtain additional experimental data to determine (or over determine) such parameters.

There are a number of possible ways to increase the number of independent ellipsometric measurements. One way is to use MAI ellipsometry. MIA ellipsometry has a number of advantages. It is simple, direct and non destructive i.e. does not perturb the system.

Chapter 3

Experimental Setup and Procedure

3.1 Preparation and Nature of the Sample

The sample used in the experiment is MDMO-PPV/PCBM[1:1]. It is a mixture of 1-[3-Methoxycarbonyl] Propyl-1 Phenyl-[6,6]-Metanofullerence (PCBM) and Poly[2-Methoxy-5(3',7'-dimethyloctyloxy)-1-4-Phenylene -vinelene](MDMO-PPV) with 50% by weight each. One of the components act as a donor of electrons while the other acts as an acceptor of electrons. This polymer has great application in heterojunction devices like solar cells. Such devices fabricated from Poly(P-Phenylene Vinylene)(PPV) and $C-60$ derivative PCBM are capable of power conversion efficiencies of up to 3% under solar conditions with their performance depending critically on film morphology.

The film is spin coated on glass substrate with speed of 500 rpm. This speed determines the thickness of the film coated on the substrate. One of the characteristic of MDMO-PPV/PCBM thin film is that by varying the concentration of each molecules, it is possible to fabricate a material with high absorption coefficient. This is necessary

for application in polymer cells because the film thickness of the photoactive layer should be normally between 100nm to 300nm.

3.2 Basic Principle of Operation of RAE

In a general scheme, RAE setup is shown in figure 3.1. It can be seen from the figure that a light source, which is well collimated, passes through a polarizer at an azimuthal angle P. The light will be linearly polarized after passing through the polarizer. This linearly polarized light interacts with the sample and its state of polarization is modified due to the interaction. The modified state of polarization of the light is then analyzed by the analyzer. In RAE, by varying the azimuthal angle of the analyzer A, the change of polarization of the light is characterized. The photo detector is placed after the analyzer. The photo detector detects the light flux of the light source after passing all the the optical components. The light detected by the photo detector is amplified for measurement by the lock in amplifier, which measures the rms of the signal.

3.2.1 Instrumentation of Rotating Analyzer Ellipsometry

A new rotating analyzer ellipsometer is assembled in this experiment. It is specially designed for a multiple angle of incidence ellipsometry measurement. Three nano rotators, which are controlled by the stepper motor controllers, are assembled together for this setup. The sample is placed on one of the nano rotators so that the angle of incidence varies as it rotates. The other nano rotator holds the analyzer and

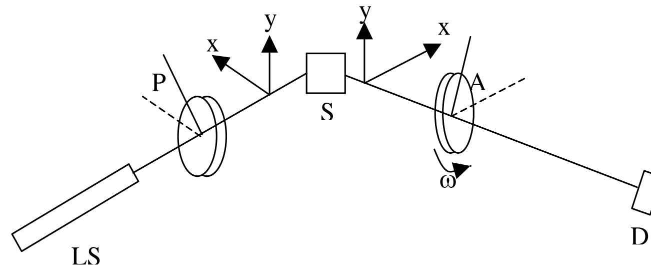

Figure 3.1: *standard rotating analyzer ellipsometer (RAE) in which polarizer is maintained at a fixed angle and compensator is absent .*

detector. As the angle of incidence is varied by rotating the sample, the analyzer and the detector traces the reflected light. This can be achieved by rotating with the speed twice that of the sample. The last nano rotator holds the analyzer. For a given angle of incidence, the analyzer is rotated by 360^0 and the ellipsometric quantities Δ and Ψ are measured. The actual setup shown in the figure(3.2) This new RAE ellipsometer has a number of advantages. As the nano rotator has a high degree of accuracy of 0.001^0, the angle of incidence and the azimuthal angle of analyzer are measured more accurately. This is very important since reflection ellipsometry is very sensitive to these measured data. A relatively small error can lead to a very erroneous results. The other advantage is that multiple angle of incidence measurement can easily be accessed using this setup. Every components are controlled by a computer so that there is no need to manually adjust for different incident angles.

Three laser sources are used in this experiment. The first one is a 5mW He-Ne laser of wavelength 632.8nm. The second one is a temperature tunable semiconductor diode laser which has a maximum output power of 450mW at wavelength 808nm.

Figure 3.2: *Automated ellipsometer setup.*

The third one is Nd:YAG laser pumped by the semiconductor diode laser and has a maximum power of 100mW at a wavelength of 1064nm. Using a KTP crystal the 1064nm laser in converted to its second harmonic frequency i.e. 532nm. The light sources are chopped by a chopper. The chopper changes the continuous light signal to a pulsed square wave. The optimum chopper frequency must be set so that the lock-in-amplifier measures only the required signal out of the ambient noise signals. The data acquisition is performed by a lock-in-amplifier which is controlled by a powerful software called LabVIEW. A lock-in-amplifier is a device which is used to detect a very small AC signal all the way down to a few nano volts. Accurate

measurement may be made even small signal is obscured by a noise sources many thousand of times larger. Lock-in-amplifier uses a technology known as phase sensitive detection to single out the component of the signal at a specific reference frequency and phase. Noise signals at frequencies other than the reference frequency are rejected and do not affect the measurement.

3.2.2 Calibration of Rotating Analyzer Ellipsometry

Reliable operation of any ellipsometer stands or fails with the accurate determination of the position of all of its component relative to the plane of incidence. [19] During calibration procedure, the position of all components relative to the plane of incidence of the sample under investigation, are determined. If this step is not taken under careful consideration, the resulting Ψ and Δ spectra are strongly affected. Hence, calibration is very critical step in the experiment.

In calibration, the correct azimuthal angle of the analyzer and the polarizer is sought. Figure 3.2 gives the azimuthal angle of the analyzer versus the intensity of the reflected light for the glass substrate. The polarizer is set at 0^0 i.e. the incident light is S-polarized. The reflected light is also S-polarized. The correct position of the analyzer gives maximum transmission at 0^0 and 180^0, and the minimum transmission at 90^0 and 270^0. This calibration is repeated for a number of times.

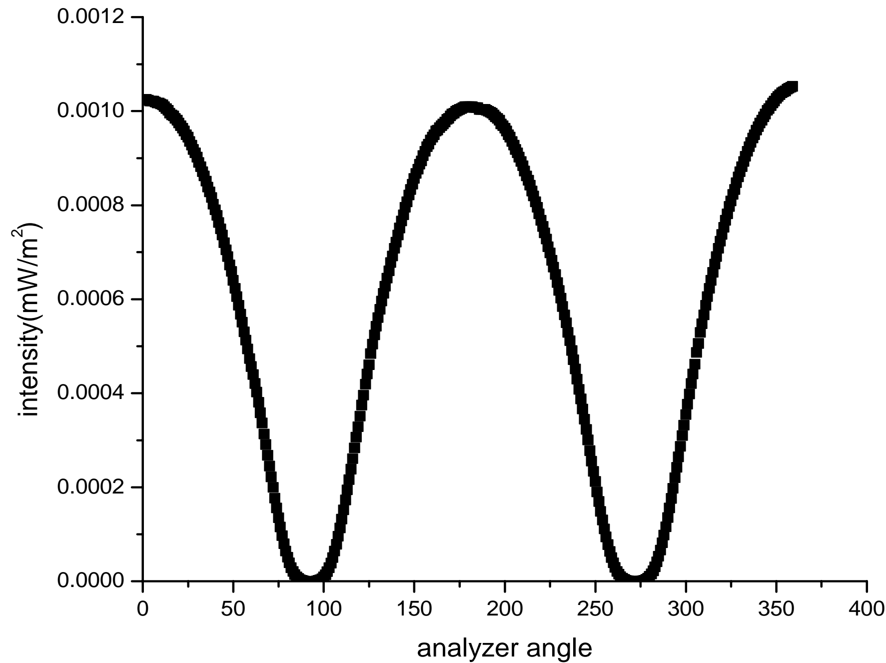

Figure 3.3: *Reflected intensity for S-polarized incident light versus analyzer angle for glass.*

3.3 Measurement and Procedure

Once the calibration is made, different measurement can be made using reflection or transmission ellipsometry. For a given substrate, the Brewster angle is measured. The procedure for the Brewster angle measurement is given below.

1. Set the polarizer at azimuthal angle P, this angle must be different from 0^0 i.e. the incident light must not be perpendicular to the plane of incidence.

2. Set the analyzer angle at 0^0

3. Rotate the sample. Here the APT(Advanced Positioning Technology) stepper motor controller user interface software that controls the stepper motors and

the LabVIEW that acquires data from the lock-in-amplifier must run simultaneously.

4. Draw the intensity versus angle of incidence.

The Brewster angle is the angle where the S-component of the reflected light vanishes. Therefore, the angle where the intensity becomes zero or minimum is sought. For glass, the index of refraction can easily be determined from Brewster angle measurement. In the case of a thin film substrate system, the index of refraction, obtained from the Brewster angle, can be used as an initial guess in the simulation programme. The other measurement made is multiple angle of incidence rotating analyzer ellipsometry. For a fixed angle of incidence, the analyzer is rotated through 360^0. The intensity versus the analyzer angle is plotted. The Fourier coefficient is obtained by fitting the curve and the ellipsometric quantities Δ and Ψ are computed. This is repeated for different angles of incidence and wavelengths.

Chapter 4

Results, Analysis and Discussion

4.1 Simulation and Numerical Inversion of Ellipsometric Data

To be able to simulate and fit Ψ and Δ spectra obtained in RAE, a model with following main features is assumed.

- A layer system is defined as a semi-infinite substrate , one layer of definite thickness and semi-infinite ambient.
- For substrate and the film , the refractive index can be definite at fixed value.
- Simulation and fits can be done as function of angle of incidence for each wavelength.
- In fitting the refractive index and the thickness, the strength are determined by minimizing the sum of the square of difference between measured and calculated values of Δ and Ψ.

When the number of unknown optical parameters of a three phase system exceed two, it is necessary to acquire additional experimental data to determine such parameters.

One way is a multiple angle of incidence measurement.

Let ρ_i^m denotes the ratio of reflection coefficients from the ith measurement on the ambient film substrate system and ρ_i^c be the computed value of the ratio of reflection coefficients. The computational task is to seek for the optical parameters (n_s, n_f, k_f and d) of the substrate and the film. This is achieved by minimizing the quantity

$$F = \sum_{i=1}^{m} \mid \rho_i^m - \rho_i^c(n_s, n_f, k_f, d, \phi_0, \lambda) \mid^2, \qquad (4.1.1)$$

where m is the number of measurements and ϕ_0 is angle of incidence. In ideal situation, F is identically zero. However, instrumental and model imperfection are unavoidable, and F has to be minimized by numerical computation. The choice of error function is not unique. An alternate error function, which deals directly with Ψ and Δ, is employed. Thus, the error function G can be defined as

$$G(\mathbf{B}) = \sum_{i=1}^{m} (\Delta_i^c(\mathbf{B}) - \Delta_i^m)^2 + (\Psi_i^c(\mathbf{B}) - \Psi_i^m)^2, \qquad (4.1.2)$$

The computational part of the problem is to find $\mathbf{B}_0$ such that the error function $G(\mathbf{B})$is minimum. $\mathbf{B}$=$(b_1, b_2, ..., b_m)$ is the parametric vector which characterizes the sample under investigation. For isotropic film on non absorbing substrate, $\mathbf{B}$=(n_f, k_f, d_f, n_s). So, the number of parameters to be determined are four. This error function is used in the numerical computation in this paper. It is generally preferable to use the error function G since the weighting involved in the error function F is unwarranted. The complete FORTRAN programme is presented in the appendix.

4.2 Parameters Correlation Test

One of the problem that a raises from numerical inversion method is that the m measurements might not give independent equations. In this case two or more parameters are correlated. The correlation between two parameters b_j and b_k occur if

$$\frac{\partial Y}{\partial b_j} = c\frac{\partial Y}{\partial b_k}$$

where c is a constant over the range of angles measured. Here Y represents either Δ or Ψ. If measurement is made at m-angles of incidence giving 2m data points (Δ and Ψ), 2m optical parameters can be determined. Mathematically, correlation reduces the number of independent equationss to less than 2m. The correlation

Angle of incidence (deg)	$\left(\frac{\partial\Delta/\partial d}{\partial\Delta/\partial nf}\right)$	$\left(\frac{\partial\Delta/\partial d}{\partial\Delta/\partial kf}\right)$	$\left(\frac{\partial\Delta/\partial ns}{\partial\Delta/\partial nf}\right)$	$\left(\frac{\partial\Delta/\partial kf}{\partial\Delta/\partial nf}\right)$
53	0.0403	0.0097	0.133	0.043
56	0.0309	0.0077	0.144	0.033
59	0.0312	0.0087	0.223	0.066
60	0.0530	0.0065	0.440	0.097
62	0.0600	0.0069	0.490	0.089

Table 4.1: *Test for the correlation of the optical parameters for MDMO-PPV/PCBM[1:1] at 532nm.*

test is performed taking the partial derivative of Δ or Ψ by varying one parameter and keeping the others constant. For five angles of incidence, the derivatives vary for wavelength 532nm(see table (4.1)). Hence, the four optical parameters (n_s, n_f, k_f, and d_f) are uncorrelated for MDMO-PPV/PCBM[1:1]. Combining data at multiple angle

of incidence at several wavelengths avoids the correlation of the parameters. This reduces the interdependence of the parameters and allows ellipsometry to determine more optical information.

4.3 Data from Brewster Angle Measurement

The intensity of the reflected light is recorded as a function of angle of incidence for both substrate and the film. At Brewster angle, the reflected electric field parallel to plane of incidence must vanish theoretically. To analyze the P-component of the electric field, transmission axis of the analyzer lies along the plane of incidence.

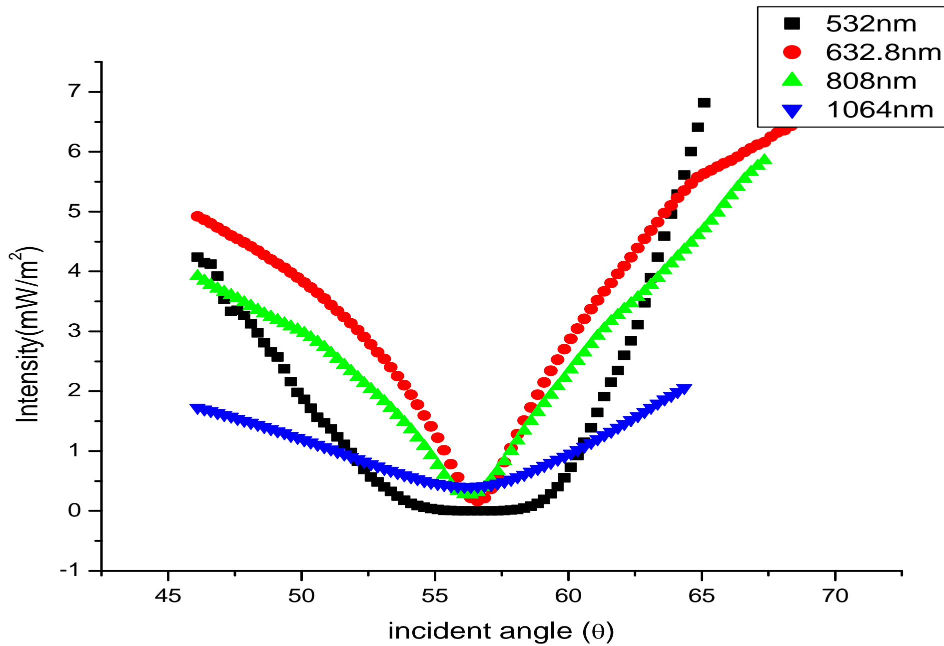

Figure 4.1: *Reflected intensity (R_p) versus analyzer angle for glass substrate .*

The index of refraction for glass substrate can be computed from Brewster angle.

$$n = tan(\theta_B), \tag{4.3.1}$$

where θ_B is Brewster angle. The Brewster angles are 56.700^0, 56.600^0, 56.350^0 and 56.100^0 for wavelengths 532nm, 632.8nm, 808nm and 1064nm respectively. The index of refraction of the glass is 1.522, 1.517, 1.502 and 1.488 for respective wavelengths.

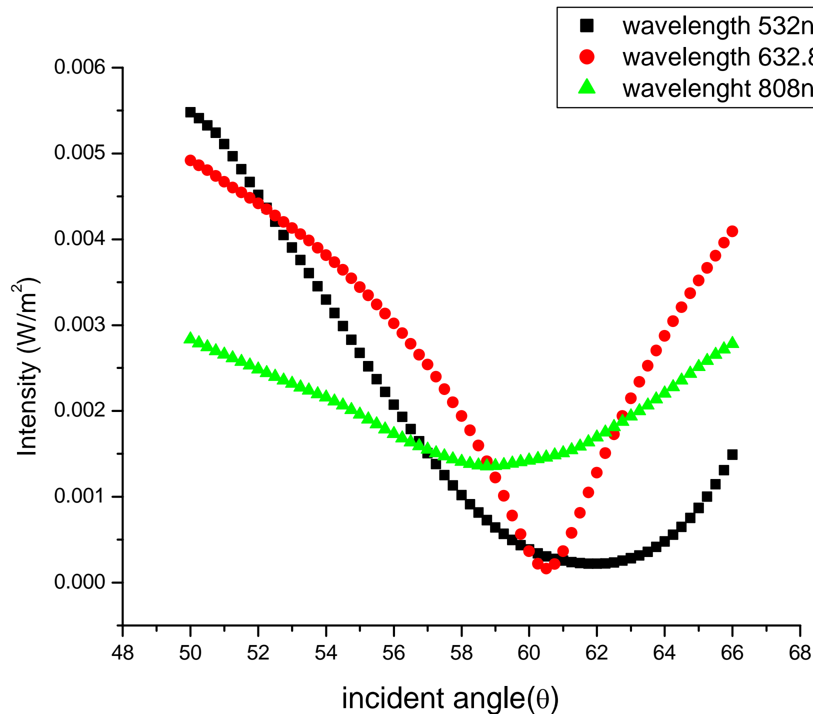

Figure 4.2: *Reflected intensity (R_p) versus angle of incidence (θ) for ambient-film-substrate .*

Similarly, the pseudo-index of refraction of the ambient-film-substrate is calculated, this can be interpreted as the index of an equivalent substrate that has the same effect as the ambient-film-substrate. This result can be used as initial guess for the

index of refraction of the film. The reflected intensity does not go to zero but attains minimum values for each wavelength. This implies that at pseudo-brewster angle of the ambient-film-substrate system, the reflected light is not completely linearly polarized. This is due to the absorbing nature of the film.

4.4 Results for Optical Parameters of MDMO-PPV/PCBM[1:1]

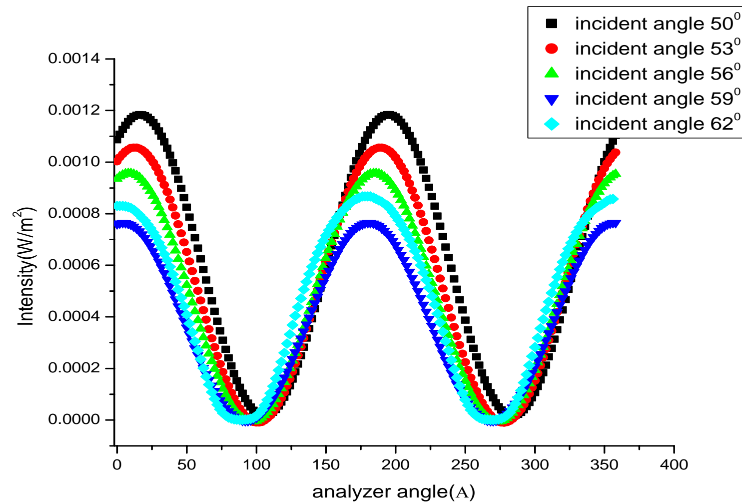

Figure 4.3: *Intensity versus analyzer angle for five angles of incidence at wavelength 532nm.*

The intensity wave forms obtained from ellipsometric measurement are sinusoidal in nature and are given by equation(2.3.7). The intensity versus analyzer angle from RAE measurements for four wavelengths are plotted(see figure 4.3, 4.7, 4.4 and 4.6).

The measured reflected intensity versus the analyzer angle is fitted with user defined equation (2.3.7) so that the Fourier coefficients a and b for the best fit are obtained. From Fourier coefficient a and b, the ellipsometric quantities Δ^m and Ψ^m

wavelength	angle	a	b	Ψ^m	Δ^m	Δ'^m	δa	δb	Ψ^c	Δ^c
	50.000	0.8101	0.5391	17.9472	156.8543	203.1457	5.60E-04	4.40E-04	17.9394	157.5029
	53.000	0.8722	0.4249	14.6413	150.3050	209.6950	9.30E-04	9.50E-04	14.7149	149.8393
	56.000	0.9183	0.2932	11.6606	137.7756	222.2244	7.70E-04	6.40E-04	11.6671	137.7700
	59.000	0.9481	0.1490	9.2702	117.9431	242.0569	6.90E-04	7.50E-04	9.2677	117.9626
532nm	62.000	0.9580	-0.0045	8.3323	89.1009	270.8991	7.90E-04	6.80E-04	8.4031	89.1173
	50.000	0.8040	0.5880	18.2426	171.4451	188.5549	9.10E-04	7.78E-04	18.2439	171.1195
	53.000	0.8718	0.4787	14.8281	167.7344	192.2656	7.60E-04	6.50E-04	14.6056	168.3988
	56.000	0.9300	0.3530	10.7818	163.8331	196.1669	9.50E-04	6.40E-04	10.7672	163.7320
	59.000	0.9716	0.2122	6.8487	153.6552	206.3448	9.20E-04	8.30E-04	6.8442	153.5433
632.8nm	62.000	0.9926	0.0594	3.4897	119.2699	240.7301	9.10E-04	6.70E-04	3.4780	119.3052
	50.000	0.8447	0.5348	16.1812	177.5947	182.4053	8.40E-04	5.50E-04	16.2308	182.3395
	53.000	0.9107	0.4119	12.1989	175.7640	184.2360	6.50E-04	7.50E-04	12.2446	183.7318
	56.000	0.9615	0.2730	7.9742	173.4749	186.5252	8.10E-04	8.40E-04	8.0325	186.6635
	59.000	0.9920	0.1210	3.6261	163.4054	196.5946	6.30E-04	7.30E-04	3.6876	196.7144
808nm	62.000	0.9983	-0.0394	1.6707	47.4688	312.5312	6.00E-04	6.60E-04	1.5933	312.5412
	50.000	0.8858	0.4589	14.6130	188.6050	171.3950	9.80E-04	9.50E-04	13.8198	188.4321
	53.000	0.9437	0.3218	9.6562	193.3577	166.6423	7.90E-04	6.70E-04	9.6511	193.2540
	56.000	0.9820	0.1706	5.4437	205.3949	154.6051	9.20E-04	9.00E-04	5.4603	205.7705
	59.000	0.9961	0.0103	2.5309	263.2961	96.7039	8.70E-04	7.30E-04	2.5177	263.2426
1064nm	62.000	0.9841	-0.1530	5.1187	329.4277	30.5723	7.70E-04	5.90E-04	5.1072	329.6318

Table 4.2: *Computed ellipsometric quantities from numerical inversion and measured ellipsometric quantities from the Fourier coefficients.*

are calculated for five angles of incidence. The simulated Δ^c and Ψ^c that give minimum error function G are sought using the numerical inversion method written in FORTRAN programme.The simulated and measured ellipsometric quantities for four wavelength is presented in table (4.2). Thus, the complex refraction of the MDMO-PPV/PCBM[1:1] film, index of refraction of the glass and thickness of the film are obtained. The results are summarized in table(4.3).

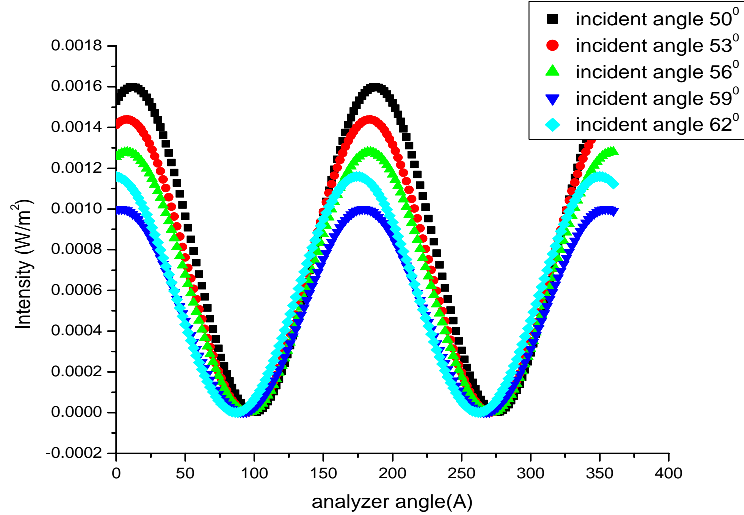

Figure 4.4: *Intensity versus analyzer angle for five angles of incidence at wavelength 808nm.*

4.5 Data from the Absorption Spectrum

As electric field wave propagates through a material,the amplitude of electric field decreases exponentially.

$$\overrightarrow{E} = \overrightarrow{E_0} e^{\frac{-\alpha z}{2}} \tag{4.5.1}$$

This implies as the wave propagates, the energy is absorbed by the material.The transmitted intensity is proportional to $\mid \overrightarrow{E} \mid^2$. Transmittance is defined as the ratio of transmitted intensity to initial intensity.

$$T = \frac{I_t}{I_0} = e^{-\alpha z}$$

where α is the absorption coefficient of the material. If we take the negative logarithm of transmission, we get the absorbance of the material.

$$A = \frac{4\pi kd}{ln(10)\lambda}, \tag{4.5.2}$$

where λ is wavelength

k is extinction coefficient of the material

d is thickness of the material

The absorbance of the polymer MDMO-PPV/PCBM[1:1] is obtained from UV/Vis

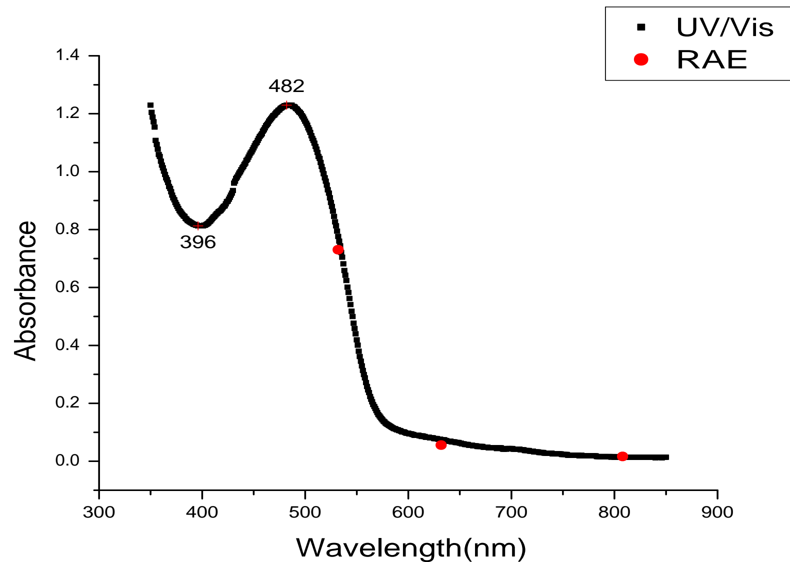

Figure 4.5: *Absorbance from UV/Vis spectrometer and Ellipsometry measurement.*

spectrometer. It has a peak value at wavelength 482nm . At this particular wavelength, the sample is highly absorbing. The absorbance decreases rapidly as the wavelength increases towards the right of the peak. In the visible range, above 600nm, the polymer is almost transparent with small value of absorbance.

Since the thickness and extinction coefficient of the polymer are determined from multiple angle of incidence ellipsometry, the absorbance at a fixed wavelength can be calculated. The two experimental results are compared. It can be seen from in graph(4.5) that the two independent measurements of absorbance are in good agreement. The slight difference arises from errors in calculating the extinction coefficient and thickness of the polymer.

4.6 Error Analysis

There are several areas of possible systematic errors in the ellipsometric measurement.

1. imperfection in polarizers results in a residual ellipticity of the light.

2. error in setting the azimuthal of the polarizing elements.

3. error in angle of incidence.

The use of high quality optical elements will reduce the effect of the incident light to insignificant levels.In this experiment high quality Glan-Thompson polarizer and analyzers are used. Hence, the error can be neglected. Error in angle of incidence can arise in the ellipsometer setup from several sources.

- error caused by beam divergence. This is a problem in Nd:YAG laser (532nm, 808nm and 1064nm). Every attempt is made to minimize beam divergence. For divergent beam, the measured values of Δ and Ψ represents an average over a range of angles of incidence.

- instrumental errors.

wavelength	Gmin	n_f	k_f	d	n_s	A	δn_f	δk_f	δd	δn_s
532nm	0.649	1.9030	0.2620	118.000	1.5190	0.1380	1.4E-3	0.3 E-3	2.24	1.5 E-3
632.8nm	0.575	1.7800	0.0230	122.000	1.5160	0.0240	1.8E-3	0.6 E-3	2.52	1.8 E-3
808nm	0.310	1.6850	0.0090	118.000	1.5100	0.0070	2.0 E-3	0.4 E-3	1.73	1.9 E-3
1064nm	0.227	1.6210	0.0020	120.000	1.4930	0.0010	2.4 E-3	0.6 E-3	1.76	1.7 E-3

Table 4.3: *measured optical constants and thickness of MDMO-PPV/PCBM[1:1].*

Computation of error function G(**B**) involves guesses for the optical parameter vector **B**. The uncertainty in the optical uncorrelated parameter b_j is calculated using the following relation.

$$\delta b_j = (\frac{2\delta G}{\partial^2 G/\partial b_j^2})^{\frac{1}{2}} \tag{4.6.1}$$

b_j can represent real refractive index, imaginary refractive index of the film or substrate or the thickness of the film. $\delta G$is the uncertainty of error function G. This results from the errors in the measured and simulated ellipsometric quantities Δ and Ψ. The denominator is a second partial derivative of the error function. Since error in the Fourier coefficients of the detected signal is known, the errors in the measured Δ and Ψ can easily be calculated from Taylor expansion.

$$\delta\Psi^m = \frac{\delta a}{2\sqrt{1-a^2}}$$

$$\delta\Delta^m = \frac{\sqrt{((1-a^2)\delta b)^2 + (ab\delta a)^2}}{1-a^2\sqrt{1-a^2-b^2}}$$

The uncertainty in G(δG)is calculated from the above uncertainties for each angle of incidence. From the numerical inversion, we can vary the error function G by varying

only one optical parameter. Then second partial derivative of G can be calculated. By applying the above procedure, the error in determined optical parameters of the sample is determined. The result is included in table (4.3). Minimum error is achieved at wavelength 632.8nm. This is due to a minimum beam divergence of the laser. For the other wavelengths the error is larger as the beam divergence in Nd:YAG laser is relatively large. The thickness of the film varies between 118 to 122 nm. This small variation, apart from computational error, might result from the difference in the morphology of the thin film at different places.

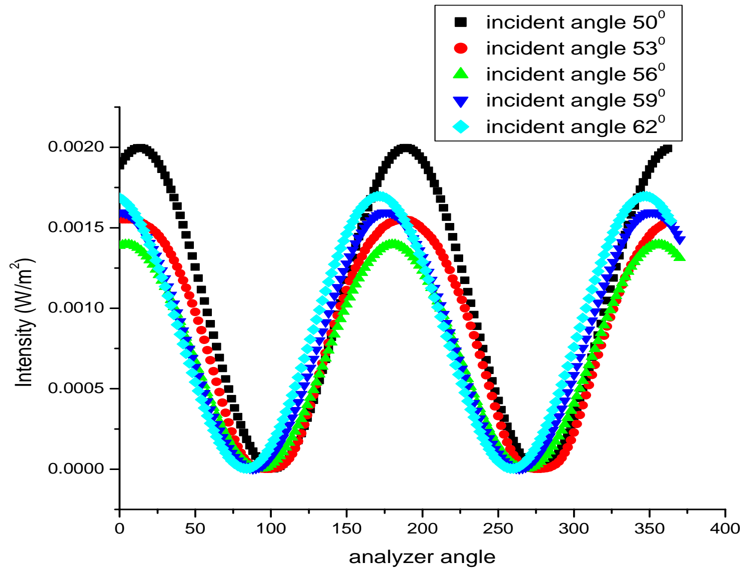

Figure 4.6: *Intensity versus analyzer angle for five angles of incidence at wavelength 1064nm.*

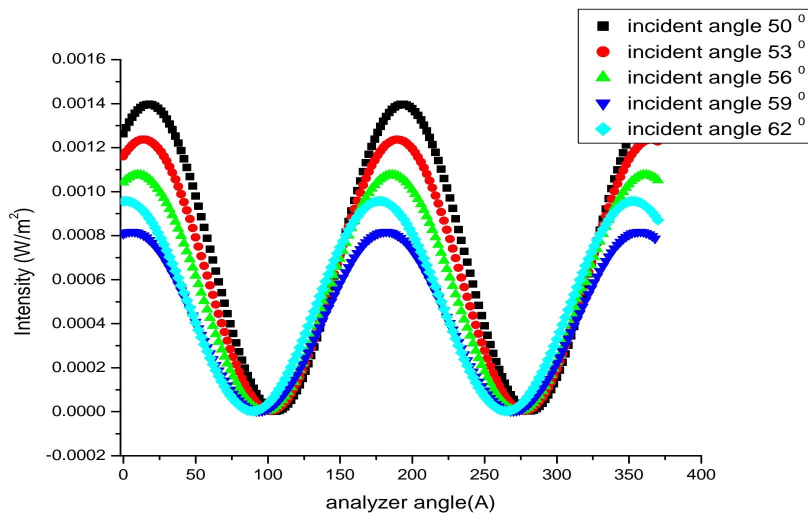

Figure 4.7: *Intensity versus analyzer angle for five angles of incidence at wavelength 632.8nm.*

Chapter 5

Conclusion and Recommendations

5.1 Conclusion

Multiple angle of incidence ellipsometry is a technique which can be used to some effect as tool for characterizing and understanding the optical properties of materials. Ellipsometry is able to measure the real and imaginary parts of refractive index, and thickness of a material simultaneously. The index of refraction of the glass substrate obtained from the Brewster angle is in good agreement with the values obtained from the optical model fitting for each wavelength. The small difference might results from the back side reflection of the glass. The thickness of the film remains almost constant with small variation(varying from 118 nm to 122 nm) for wavelength 532 nm, 632.8 nm, 808 nm, and 1064nm. The thickness measured from spin coating is in the range 100 nm-140 nm. Hence, the result obtained from MAI measurement is with in this range. The complex refractive index of the sample is determined to be 1.9030-i0.2620, 1.7800-i0.0230, 1.6850-i0.0090 and 1.621-i0.0020 for wavelength 532 nm, 632.8 nm, 808 nm and 1064 nm. The index of refraction decreases as the wavelength increases implying that the dispersion is normal for wavelength range used in the experiment. Further attempt was made to correlate data obtained from

the absorption and the MAI ellipsometric measurements. The agreement of the two measurements further strengthens the reliability of the results obtained from MAI ellipsometric measurement.

5.2 Recommendations

Improved calibration procedure

A very critical step in ellipsometry measurement is the calibration procedure.It is more or less the same as finding the global extreme of a multi-dimensional function. In this experiment, glass is used for calibration purpose. Back side reflection from the glass makes the calibration process difficult. Therefore, different substrate like gold should be used to improve the calibration of the ellipsometer.

Integrated ellipsometer

In current implementation, four wavelengths are only used for MAI ellipsometry measurement. This gives only four different experimental data over range of wavelengths spectrum. Combining data at a multiple angle of incidence at several wavelengths can reduce the interdependence of the optical parameters and allow ellipsometry to determine more optical information than either multiple angle of incidence or spectroscopic ellipsometry on their own alone. Further interfacing is demanded to integrate the monochrometer, stepper motors and lock-in-amplifier.

Appendix

```
! Numerical inversion iteration for mutiple angle of incidence ellipsometry.
  This programe fits optical parameters of the sample that gives minimum error

function.

   COMPLEX nf,a,b,c,ro1p,r12p,ro1s,r12s,img,RP,RS,beta
   COMPLEX rho(100)
   REAL psic(10),deltc(10),g(10),rrho(10),lamd(10),angl(10)
   REAL irho(10),psim(10),delm(10),delm1(10),g1(10)
   REAL ns,n0,d,e,a1,kf,kfi,kff,a1i,a2i,a2f,delt1,delt2,delt3,n,m,nsi,nsf,i,deltn1
   img=CMPLX(0,1)
   OPEN(1,FILE='akl3.dat',STATUS='unknown')
   OPEN(2,FILE='akl808.dat',STATUS='unknown')
   OPEN(16,FILE='outp808.dat',STATUS='unknown')

   PRINT*,' Enter the number of measurements and differrent wavelegths used'
   READ*,m,n
   PRINT*,'Enter the error g minimum '!g is the error function chosen
   READ*,e
   !Reads the angle of incidence and the measured ellipsometric quantities for

each wavelength

    do k=1,n
        READ(1,*) lamd(k)    !Reads the wavelength from file 1
      do i=1,m
         READ(2,*)angl(i+(k-1)*m),psim(i+(k-1)*m),delm(i+(k-1)*m),delm1(i+(k-1)*m)
      end do
    end do
```

```
do k=1,n     !k specifies different wavelengths

        PRINT*,'enter the initial guess of the optical parameters for
wavelength',lamd(k),'in the

order given'
        PRINT*,'enter index of refraction of the substrate nsi(starting) and
nsf(ending)

iteration'
        READ*,nsi,nsf
        PRINT*,'enter real part of index of refraction of the film nfi(starting) and
nff(ending)

iteration'
        READ*,a1i,a1f
        PRINT*,'enter imaginary part of index of refraction of the film
kfi(starting) and

kff(ending) iteration'
        READ*,kfi,kff
        PRINT*,'enter thickness di(starting),df(final)'
        READ*,di,df
        PRINT*,'the output  values for wavelength',lamd(k),'are:'
        WRITE(16,*)'wavelength',lamd(k)

     delt1=0.001 ! increment index of refraction of a substrate
     delt2=0.001 ! increment the extinction coefficient of the film
     deltn1=.001 !  increment the real index of refraction of the film
     delt3=1     ! increment thickness of the film
     n0=1 ! index of refraction of air

  do ns=nsi,nsf,deltn1   !iterates the index of refraction of a substrate
   do a1=a1i,a1f,delt1   !iterates the real index of refraction of the film
    do kf=kfi,kff,delt2  !iterates the extinction coefficient of the film
     do d=di,df,delt3    !iterates the thikness of the film
        nf=CMPLX(a1,-kf) !assigns  the complex refractive index of the film

      do i=1,m           !iterates the error function g for m measurements

           a=COS(angl(i+(k-1)*m))
           b=SQRT(1-(n0*SIN(angl(i+(k-1)*m))/nf)**2)
           c=SQRT(1-(n0*SIN(angl(i+(k-1)*m))/ns)**2)
           beta=8*d*ATAN(1.0)*b*nf/lamd(k)
           ro1p=(nf*a-n0*b)/(nf*a+n0*b)
           r12p=(ns*b-nf*c)/(ns*b+nf*c)
           ro1s=(n0*a-nf*b)/(n0*a+nf*b)
           r12s=(nf*b-ns*c)/(nf*b+ns*c)
           RP=(ro1p+r12p*EXP(-img*2*beta))/(1+ro1p*r12p*EXP(-img*2*beta))
           RS=(ro1s+r12s*EXP(-img*2*beta))/(1+ro1s*r12s*EXP(-img*2*beta))
           rho(i)=RP/RS
           rrho(i)=REAL(rho(i))
           irho(i)=AIMAG(rho(i))
           psic(i)=45*ATAN(SQRT(rrho(i)**2+irho(i)**2))/(ATAN(1.0))
           deltc(i)=45*ATAN(irho(i)/rrho(i))/(ATAN(1.0))
   ! the cases below determine the quadrant of the angle 'delta'

           if(rrho(I)<=0.and.irho(i)<0) then
               deltc(i)=deltc(i)+180
           end if
```

```
          if(rrho(i)<0.and.irho(i)>=0)then
              deltc(I)=deltc(i)+180
          endif

          if(rrho(i)>=0.and.irho(i)<=0)then
             deltc(I)=deltc(i)+360
          end if

          if(rrho(I)>0.and.irho(I)>=0) then
            deltc(I)=deltc(I)
          end if

           g(1)=0.0          !assigns the initial error function g to zero
           g1(1)=0.0
  !delta can have two values delm or delm1= 360-delm
           g(i+1)=(delm(i+(k-1)*m)-deltc(i))**2+(psim(i+(k-1)*m)-psic(i))**2
            g1(i+1)=(delm1(i+(k-1)*m)-deltc(i))**2+(psim(i+(k-1)*m)-psic(i))**2
            g(i+1)=g(i)+g(i+1) ! sum the error function g for m mesurement for delm
           g1(i+1)=g1(i)+g1(i+1) !sum the error function g for m mesurement for delm
       end do
  !selects  minimum g or g1 for iterated parameters
         If(g(m+1)<=e.or.g1(m+1)<=e)then
  !prints the optical parameters that minimizes the error function
         PRINT*,g1(m+1),g(m+1),a1,d,kf,ns
  !writes the optical parameters that minimizes the error function on a file
         WRITE(16,*)g1(m+1),g(m+1),a1,d,kf,ns
       endif

      end do
     end do
   end d0
  end do
 end do
end
```

The initial guess of the optical parameters of the sample that is fed to programme is presented in the following table

Wavelength(nm)	nf	kf	ns	d(nm)
532	1.900-2.000	0.100-0.300	1.519-1.526	100-300
632.8	1.760-2.000	0.050-0.300	1.514-1.530	100-300
808	1.650-2.000	0.006-0.010	1.510-1.520	100-300
1064	1.620-2.000	0.002-0.010	1.490-1.520	100-300

Bibliography

[1] E.Hecht, *Optics*, 4th ed., Addison-Wesley, New York (1974)

[2] W.A.Bashara and S.S.Shurcliff, *Polarized Light*, 2nd ed., Elselvier: Amsterdam (2003).

[3] E.Hecht and A.Zajac, *Optics*, chap.8, p.266, Addison-Wesley,New York (1974)

[4] S.S.Ballard and W.A.Shurcliff, *Polarized Light*,Van Nostrand,Princeton,N.J (1964)

[5] R.M.A.Azzam and N.M.Bashara, *Ellipsometry and polarized light*, chap.2, p.148, 2nd ed., Elselvier: Amsterdam (2003).

[6] J.W.Hovenier,"Structure of a general pure Mueller matrix" *Appl.Opt.***33**, 8318-8324 (1994).

[7] R.M.A.Azzam and N.M.Bashara, *Ellipsometry and polarized light*, chap.3, p.153, 2nd ed., Elselvier: Amsterdam (2003).

[8] R.M.A.Azzam, "Ellipsometry," in W.L.Wolfe(ed.), *Handbook of Optics*, 2nd ed., vol.II, chap.27, p.27, McGraw-Hill, New York (1995).

[9] R.A Chipman, *Handbook of Optics*, 2nd ed., vol.II, chap.22, p.22, McGraw-Hill, New York (1975).

[10] H.C.vzn de Hulst, *Light Scattering by Small Particles*, chap.5, p.44, John Wiley & Sons, New york (1957).

[11] M.Born and E.Wolf, *Principles of Optics*, chap.1, p.40 (1959)

[12] R.M.A.Azzam and N.M. Bashara, *Ellipsometry and polarized light*, chap.4, p.286, 2nd ed., Elselvier: Amsterdam (2003).

[13] D.E.Aspnes, "Fourier transform detection system for rotating analyzer ellipsometer," *Opt.Comm.* **8**, 222-225 (1973).

[14] P.S.Hauge and F.H. Dill, " A rotating- compensator Fourier ellipsometer," *Opt.Comm.***14**, 431-437 (1975)

[15] S.N.Jasperson and S.E Schanatterly, "An improved method for high reflectivity ellipsometry based on a new polarization modulation technique," *Rev.Sci.Instr.***40**, 761-767 (1969) .

[16] R.M.A.Azzam and N.M. Bashara , *Ellipsometry and polarized light*, chap.3, p.257, 2nd ed., Elselvier: Amsterdam (2003).

[17] T.E Jenkins, "Multiple-angle-of-incidence ellipsometry," *J.Phys.D:Appl.Phys.***32** (1998).

[18] R.M.A.Azzam and N.M. Bashara , *Ellipsometry and polarized light*, chap.4, p.317, 2nd ed., Elselvier: Amsterdam (2003).

[19] J.M.M. de Nijs, A.H.M.Holtslag,A.Hoekstra, and A.van Silfhout," A new calibration method for rotationg analyzer ellipsometer," *J. Opt. Soc. Am. A* **5**, 1466 (1988)